

BUILDING EDGE EXTRACTION FROM LIDAR BASED ON JUMP DETECTION IN NON-PARAMETER REGRESSION MODEL

J. Li^{a,*}, Y. Li^a, M. A. Chapman^b

^a Department of Geography, University of Waterloo, Waterloo, N2L 3G1 CANADA, {junli, y62li}@fes.uwaterloo.ca

^b Department of Civil Engineering, Ryerson University, Toronto, M5B 3K3 CANADA, mchapman@ryerson.ca

KEY WORDS: LIDAR data, Jump Point, Building extraction.

ABSTRACT:

Light Detection and Ranging (LIDAR) technology has received great attention due to its ability to accurately measure the shape and height of objects suitable for a large range of applications such as generating Digital Elevation Models (DEM's) and modelling 3D city environment. The buildings are of particular interest due to their usefulness in 3D city modelling. Several techniques have been used to extract building with LIDAR systems. In this paper, the task of extracting significant built edge in raster LIDAR data is studied. The implemented method takes advantage of the detection of jump points in nonparametric models since points of building edges in LIDAR data usually describe sudden local changes, called jump points. Firstly, the LIDAR pixels are represented as observations from a regression model with identical distributed random errors with mean 0 and variance σ^2 in order to transform the extraction of building edge point problem into a nonparametric regression problem. Then the jump points corresponding to the building edge in the nonparametric regression model are detected by a locally weighted estimator. Finally, by a post ping procedure the thinning building edges are extracted. This algorithm has been examined by a set of simulated LIDAR data. The results show the efficiency of the proposed algorithm for extracting building edges in complex city environments.

1. INTRODUCTION

Light Detection and Ranging (LIDAR) is a rapidly emerging technology in photogrammetry, remote sensing, surveying and mapping communities, which provides high accurate Earth's surface contour information (Ackermann, 1999; Baltsavias, 1999a, b, c; Wehr and Lohr, 1999). A typical LIDAR system consists of a platform (e. g., helicopter or aircraft) and a scanning laser sensor. The position of the sensor onboard the aircraft is monitored by global positioning system (GPS) and inertial navigation system (INS). The scan angle of the laser beam can also be obtained at each instant of data collection. The range (or distance) from the sensor to the location on the Earth's surface is recorded by a laser beam. It can be expressed as followings, $D = g(s, t, \Theta)$, where D is the distance from sensor to the surface location, s denotes spatial location on the Earth's surface, t means temporal variable, Θ represents the set of angles that specify the geometric configuration of environmental object and sensor.

The need for topographic information about the Earth's surface and objects on it has been increasing considerably over the past few years, at all levels of detail and precision. It arises from a growing number of applications of such information to various fields such as agriculture (Carsjens and Knaap, 2002), forest (Treitz and Howarth, 2000), geology (King, 2001), hydrology (Schmugge et al., 2002), environment (Lee and Kwan, 2005), transportation (Demirel, 2004), urban planning (Masser, 2001;

Maktav et al., 2005), and so on. It should be noted that some issues in topographic information extraction are still open, especially with respect to data analysis, representation and fusion. Much work is needed, especially, for building, road, and tree extraction both to model 3D city environment and to find digital terrain model (DTM) of the ground.

In the current years, LIDAR is widely applied in 3D object extraction. A variety of different methods have been proposed for this purpose, some of which can be found from Tao and Hu (2001). Baltsavias *et al.* (1995) discussed three different approaches, namely using an edge operator, mathematical morphology, and height bins for detection of objects higher than the surrounding topographic surface. These main approaches were also used by other authors like Haala and Brenner (1999), and Eckstein and Munkelt (1995). They analyzed the compactness of height bins, or used mathematical morphology (Eckstein and Munkelt, 1995; Hug, 1997). Hug (1997) applied mathematical morphology in order to obtain an initial segmentation, and the reflectance data were used to discern man-made objects from natural ones via a binary classification. Other building extraction methods include the extraction of planar patches, some of which used height, slope and/or aspect images for segmentation (e. g., Haala and Brenner, 1999; Morgan and Tempfli, 2000; Morgan and Habib, 2002). In general, these methods can be grouped into two categories (Yoon *et al.*, 2002): classification approach and adjustment approach. The classification approach detects the

* Corresponding author. Dr. Prof. Jonathan Li, Department of Geography, University of Waterloo, 200 University Avenue West, Waterloo, Ontario, Canada, N2L 3G1, junli@fesmail.uwaterloo.ca.

ground points using certain operators designed based on mathematical morphology (Vosselman, 2000) or terrain slope (Axelsson, 1999) or local elevation difference (Wang *et al.*, 2001). Refined classification approach used triangulated irregular network (TIN) data structure (Axelsson, 2000; Vosselman and Mass, 2001) and iterative calculation (Axelsson, 2000; Sithole, 2001) to consider the discontinuity in LIDAR data or terrain surface. The adjustment approach essentially uses a mathematical function to approximate the ground surface, which is determined in an iterative least adjustment process while outliers of non-ground points are detected and eliminated (Kraus and Pfeifer, 1998, 2001; Schickler and Thorpe, 2001). Although much more efforts have been made in 3D data analysis over urban environment, difficulties still remain. For example, the DTM generation from LIDAR data is not yet mature (Vosselman and Maas, 2001; Yoon *et al.*, 2002). It has been realized by many photogrammetrists that methods based on single terrain characteristic or criterion can hardly obtain satisfactory results in all terrain types.

The research in this paper deals with building extraction from LIDAR data by using techniques based on non-parameter regression model. The implemented method takes advantage of the detection of jump points in nonparametric models since points of building edges in LIDAR data usually describe sudden local changes, called jump points. Firstly, the LIDAR pixels are represented as observations from a regression model with identical distributed random errors with mean 0 and variance σ^2 in order to transform the extraction of building edge point problem into a nonparametric regression problem. Then the jump points corresponding to the building edge in the nonparametric regression model are detected by a locally weighted estimator. Finally, by a post ping procedure the thinning building edges are extracted.

The organization of the paper is as follows. Section 2 describes the proposed algorithm. The result and experiment are shown in the section 3. Section 4 summarizes the conclusions on the proposed jump detection algorithm for building extraction.

2. DESCRIPTION OF ALGORITHM

Assumption: n^2 observations $\{(x_i, y_j, Z_{ij}), i, j = 1, 2, \dots, n\}$ are generated from the regression model,

$$Z_{i,j} = f(x_i, y_j) + \varepsilon_{i,j} \quad (1)$$

where f is bivariate regression function and $\{\varepsilon_{ij}, i, j = 1, 2, \dots, n\}$ are independent and identical distributed random errors with mean 0 and variance σ^2 .

For any point (x_i, y_j) for $i, j = 1, 2, \dots, n$ its linear neighborhoods, $X_i(x_i, y_j)$ and $Y_j(x_i, y_j)$, being along x and y directions with the length $k = 2l+1$, where l is a nonnegative integer, are defined by

$$X_i(x_i, y_j) = \{(x_{i+s}, y_j), s = -l, -l+1, \dots, 0, \dots, l-1, l\} \quad (2)$$

$$Y_j(x_i, y_j) = \{(x_i, y_{j+t}), t = -l, -l+1, \dots, 0, \dots, l-1, l\} \quad (3)$$

which are segments including k points, respectively. The Figure 1 illustrates the definition of neighbourhoods.

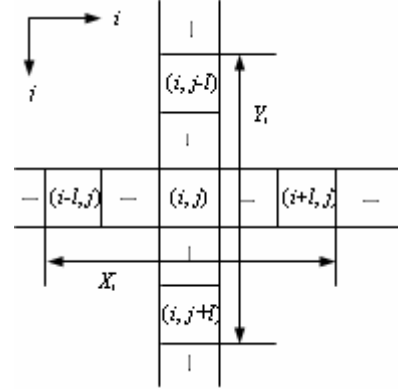


Figure 1. Illustration of neighbours

Least squares (LS) lines are then fitting in these neighbourhoods is given by

$$\begin{cases} \hat{Z}_i = \hat{a}_i + \hat{b}_i(x - x_i) \\ y = y_j \end{cases} \quad (4)$$

where $(x, y) \in X_i(x_i, y_j)$,

$$\hat{a}_i = \frac{1}{k} \sum_{s=-l}^l Z_{i+s,j}$$

$$\hat{b}_i = \frac{1}{S_i^2} \sum_{s=-l}^l (x_{i+s} - x_i) Z_{i+s,j}$$

$$S_i^2 = \sum_{s=-l}^l (x_{i+s} - x_i)^2$$

$$\begin{cases} x = x_i \\ \hat{Z}_j = \hat{a}_j + \hat{b}_j(y - y_j) \end{cases} \quad (5)$$

where $(x, y) \in Y_j(x_i, y_j)$

$$\hat{a}_j = \frac{1}{k} \sum_{t=-l}^l Z_{i,j+t}$$

$$\hat{b}_j = \frac{1}{S_j^2} \sum_{t=-l}^l (y_{j+t} - y_j) Z_{i,j+t}$$

$$S_j^2 = \sum_{t=-l}^l (y_{j+t} - y_j)^2$$

Neighbourhoods $X_{i+k}(x_{i+k}, y_j)$, $X_{i-k}(x_{i-k}, y_j)$, $Y_{j+k}(x_i, y_{j+k})$ and $Y_{j-k}(x_i, y_{j-k})$ centered the points (x_{i+k}, y_j) , (x_{i-k}, y_j) , (x_i, y_{j+k}) and (x_i, y_{j-k}) are defined, respectively,

$$X_{i+k}(x_{i+k}, y_j) = \{(x_{i+k+s}, y_j), s = -l, -l+1, \dots, 0, \dots, l-1, l\} \quad (6)$$

$$X_{i-k}(x_{i-k}, y_j) = \{(x_{i-k+s}, y_j), s = -l, -l+1, \dots, 0, \dots, l-1, l\} \quad (7)$$

$$Y_{j+k}(x_i, y_{j+k}) = \{(x_i, y_{j+k+i}), t = -l, -l+1, \dots, 0, \dots, l-1, l\} \quad (8)$$

$$Y_{j-k}(x_i, y_{j-k}) = \{(x_i, y_{j-k+i}), t = -l, -l+1, \dots, 0, \dots, l-1, l\} \quad (9)$$

In above neighborhoods, LS lines are fitted as done in $X_i(x_i, y_j)$ and $Y_j(x_i, y_j)$. And let the slopes of the fitted lines in $X_{i+k}(x_{i+k}, y_j)$, $X_{i-k}(x_{i-k}, y_j)$, $Y_{j+k}(x_i, y_{j+k})$ and $Y_{j-k}(x_i, y_{j-k})$ be \hat{b}_{i+k} , \hat{b}_{i-k} , \hat{b}_{j+k} and \hat{b}_{j-k} , respectively.

Thus the jump detection criterion is defined as follows:

$$\delta_{ij} = \max\{\min\{|\hat{b}_{i+k} - \hat{b}_i|, |\hat{b}_i - \hat{b}_{i-k}|\}, \min\{|\hat{b}_{j+k} - \hat{b}_j|, |\hat{b}_j - \hat{b}_{j-k}|\}\} \quad (10)$$

A large value of δ_{ij} indicates a possible edge at (x_i, y_j) . In order to determinate possible edges, a threshold value for δ_{ij} is necessary. In Equation (10), without loss of generality, we assume that

$$\min\{|\hat{b}_{i+k} - \hat{b}_i|, |\hat{b}_i - \hat{b}_{i-k}|\} \geq \min\{|\hat{b}_{j+k} - \hat{b}_j|, |\hat{b}_j - \hat{b}_{j-k}|\} \quad (11)$$

For any constant $c > 0$, it can be obtained that

$$\begin{aligned} P(\delta_{ij} > c) &= P(\min\{|\hat{b}_{i+k} - \hat{b}_i|, |\hat{b}_{i-k} - \hat{b}_i|\} > c) \\ &\leq P(|\hat{b}_{i+k} - \hat{b}_i| > c) = P(|\hat{b}_{i+k} - \hat{b}_i|^2 > c^2) \quad (12) \\ &= E\left\{P\left(|\hat{b}_{i+k} - \hat{b}_i|^2 > c^2 \middle| \hat{b}_i\right)\right\} \end{aligned}$$

For fixed \hat{b}_i , $\frac{|\hat{b}_{i+k} - \hat{b}_i|^2}{\sigma_{X_{i+k}}^2}$ is approximately χ_1^2 distributed under the assumption that there is no jump in $X_{i+k}(x_{i+k}, y_j) \cup X_i(x_i, y_j)$, where $\sigma_{X_{i+k}}^2 = \text{Var}(\hat{b}_{i+k}) = \frac{\sigma^2}{S_{i+k}^2}$. Therefore, a natural threshold value for δ_{ij} is

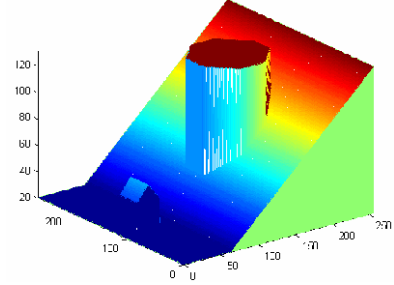
$$c = \sqrt{\chi_{1,1-\alpha}^2 \frac{\hat{\sigma}^2}{S_{i+k}^2}} \quad (13)$$

where $\chi_{1,1-\alpha}^2$ is a $1-\alpha$ quantile of the χ_1^2 distribution and $\hat{\sigma}^2$ is a consistent estimator of σ . According to the threshold defined above, the pixel point (x_i, y_j) is defined as edge point of an object if $\delta_{ij} > c$ is satisfied.

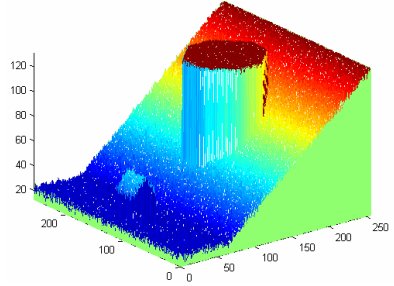
3. EXPERIMENTS AND RESULTS

The proposed building edge detection algorithm is examined with simulated data. The regression surface is designed as

landscape with plane continued a slope for $(x, y) \in [0, 255] \times [0, 255]$ and a house and a high building on the plane and slope respectively as shown in Figure 2a. Then this surface has two jump local edges around the house and the building respectively. The $256 \times 256 = 65536$ observations $\{Z_{ij}, i, j = 0, 1, \dots, 255\}$ are generated from the regression surface with the identical distributed random errors, $\varepsilon_{ij} \sim N(0, 0.5^2)$ as shown in Figure 2b.



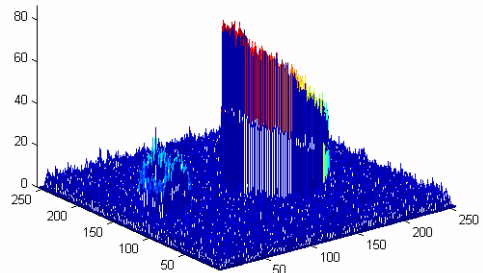
(a)



(b)

Figure 2. (a) ideal regression surface, (b) 65536 sampling points of the regression surface with noise.

The edge detection criterion δ_{ij} is then calculated by Equation (10) with $k = 1$ is plotted in Figure 3a (a 3D plot) and Figure 3b (a corresponding image plot). In the image plot, the brightness at each pixel represents the respond value: the darker, the bigger. Clearly the criterion δ_{ij} does have some ability to reveal the jump edges.



(a)

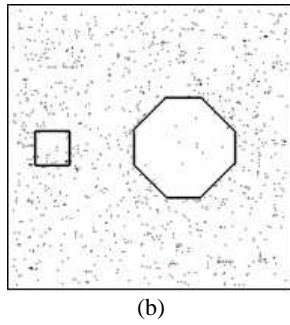


Figure 3. (a): The jump edge detection criterion (δ_{ij}) in 3D plot; (b): The corresponding image plot of (a), the darker the colour in the image, the bigger the criterion value of δ_{ij} .

In order to extract the clear jump edges, some post-processing procedures are employed. In this study, the edge of a building is modeled as a combination of line-like segments and the direct morphological dilation operation developed in our previous work is used to extract these line-like segments from image for δ_{ij} . The Figure 4a shows the result from the direct morphological dilation operation to image in Figure 3b. In this study, a thinning edge operation designed in our previous work is also used to obtain exact edges, see Figure 4b.

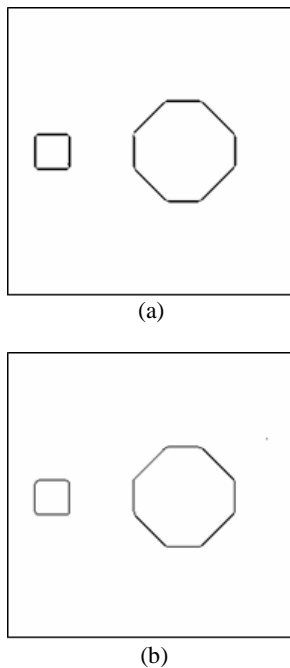


Figure 4. (a) The edges of jump changes from directly morphological operation to image in Figure 3b, (b) The thinning edges for (a).

The proposed algorithm is also exercised to extract roof edges from raw LIDAR data. Figure 5 shows the rasterized LIDAR image by using nearest neighbourhood algorithm.

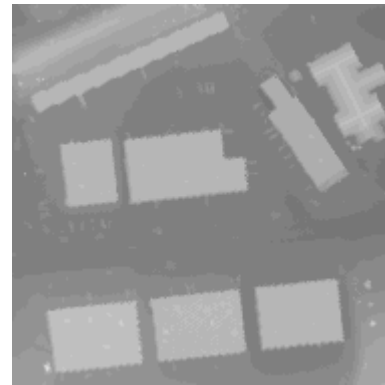


Figure 5. Raster LIDAR image.

The result from the proposed building extraction algorithm is shown in Figure 6.

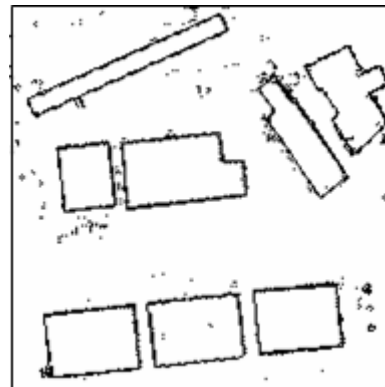


Figure 6. Extracted building outlines

This extracted building outline image is filtered by directed morphological operations, as shown in Figure 7.

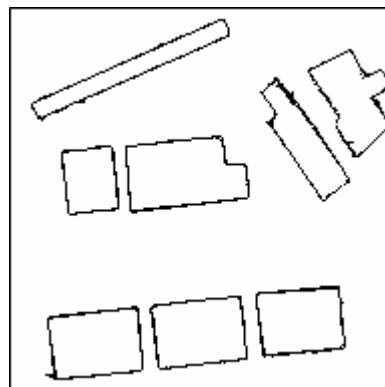


Figure 7. Filtering Building outline image.

The filtering outline image is further thinned by a thinning algorithm, see Figure 8.

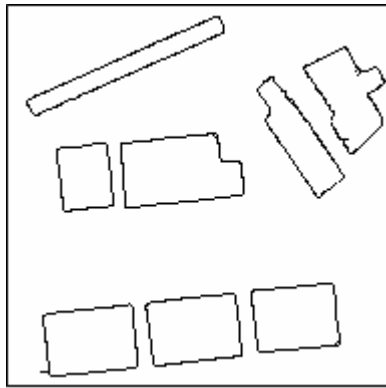


Figure 8. Thinning building outline image.

In order to demonstrate the accurate for extracted building outline, the thinning outlines of extracted buildings are overlaid on the original image, as shown in Figure 9.



Figure 9. Overlay the building outlines on the original image.

4. CONCLUSIONS

In this paper, the task of extracting significant built edge in raster LIDAR data is studied. The implemented method takes advantage of the detection of jump points in nonparametric models since points of building edges in LIDAR data usually describe sudden local changes, called jump points. This algorithm has been examined by a set of simulated LIDAR data. The results show the efficiency of the proposed algorithm for extracting building edges in complex city environments.

ACKNOWLEDGEMENTS

The research was partially supported by a Natural Sciences and Engineering Research Council of Canada (NSERC) discovery grant. The PhD research scholarship provided by the School of Graduate Studies at University of Waterloo is also acknowledged.

REFERENCE

- Ackermann, F., 1999. Airborne laser scanning: present status and future expectations. *ISPRS Journal of Photogrammetry and Remote Sensing*, 54(2-3): 64-67.
- Axelsson, P., 1999. Processing of laser scanner data: algorithms and applications. *ISPRS Journal of Photogrammetry and Remote Sensing*, 54(2-3): 138-147.
- Axelsson, P., 2000. DEM generation from laser scanner data using adaptive TIN models. *International Archive of Photogrammetry and Remote Sensing*, 33 (B4): 110-117.
- Baltsavias, E. P., 1995. Use of DTMs/DSMs and orthoimages to support building extraction. In *Automatic Extraction of Man-Made Objects from Aerial and Space Images*, Gruen, A. and O. A. P. Kubler (Eds.), Birkhaeuser, Basel.
- Baltsavias, E. P., 1999a. A comparison between photogrammetry and laser scanning. *ISPRS Journal of Photogrammetry and Remote Sensing*, 54(2-3): 83-94.
- Baltsavias, E. P., 1999b. Airborne laser scanning: existing systems and firms and other resources. *ISPRS Journal of Photogrammetry and Remote Sensing*, 54(2-3): 164-198.
- Baltsavias, E. P., 1999c. Airborne laser scanning: basic relations and formulas. *ISPRS Journal of Photogrammetry and Remote Sensing*, 54(2-3): 199-214.
- Carsjens, G. J. and W. van der Knaap, 2002. Strategic land-use allocation: dealing with spatial relationships and fragmentation of agriculture. *Landscape and Urban Planning*, 58(2-4): 1717-179.
- Demirel, H., 2004. A dynamic multi-dimensional conceptual data model for transportation applications. *ISPRS Journal of Photogrammetry and Remote Sensing*, 58(5-6): 301-314.
- Eckstein, W. and O. Munkelt, 1995. Extracting objects from digital terrain models. In *Remote Sensing and Reconstruction for Three-Dimensional Objects and Scenes*, Schenk, T. (ed.), San Diego.
- Haala, N. and C. Brenner, 1999. Extraction of buildings and trees in urban environments. *ISPRS Journal of Photogrammetry and Remote Sensing*, 54(2-3): 130-137.
- Hug, C., 1997. Extracting artificial objects from airborne laser scanner data. In *Automatic Extraction of Man-Made Objects from Aerial and Space Images (II)*, Gruen, A., E. Baltsavias and O. Henricsson (eds.), Birkhaeuser, Basel.
- King, R. B., 2001. *Remote Sensing Geology*, John Wiley, New York, USA.
- Kraus, K. and N. Pfeifer, 2001. Advanced DEM generation from LiDAR data. *International Archives of the Photogrammetry, Remote Sensing and Spatial Information Sciences*, 34(3/W4).
- Lee, J. and M. P. Kwan, 2005. A combinatorial data model for representing topographic relations among 3D geographical features in micro-spatial environments. *International Journal of Geographical Information Science*, 19(10): 1039-1056.

- Maktav, D., F. S. Erbek and C. Jürgens, 2005. Remote sensing of urban areas. *International Journal of Remote Sensing*, 26(4): 655-659.
- Masser, I., 2001. Managing our urban future: the role of remote sensing and geographic information systems. *Habitat International*, 25(4): 503-512.
- Morgan, M. and A. Habib, 2002. Interpolation of LiDAR data and automatic building extraction. *ASPRS Annual Conference* (CD-ROM), Washington, DC, April 19–25, 2002.
- Morgan, M. and K. Tempfli, 2000. Automatic building extraction from airborne laser scanning data. *International Archives of Photogrammetry and Remote Sensing*, 33 (B3): 616–623.
- Schickler, W. and A. Thorpe, 2001. Surface estimation based on LiDAR. *Proceedings of ASPRS Annual Conference* (CD-ROM), April 23-27, 2001, St. Louis, Missouri, USA.
- Schmugge, T. J., W. P. Kustas, J. C. Ritchie, T. J. Jackson and A. Rango, 2002. Remote sensing in hydrology. *Advances in Water Resources*, 25(8-12): 1367-1385.
- Sithole, G., 2001. Filtering of laser altimetry data using slope adaptive filter. *International Archives of Photogrammetry and Remote Sensing*, 34(3/W4): 203-210.
- Tao, C. and Y. Hu, 2001. A review of post-processing algorithms for airborne LiDAR data. *Proceedings of SPRS Annual Conference* (CD-ROM), April 23–27, St. Louis, Missouri, USA.
- Treitz, P. and P. Howarth, 2000. High Spatial Resolution Remote Sensing Data for Forest Ecosystem Classification: An Examination of Spatial Scale. *Remote Sensing of Environment*, 72(3): 268-289.
- Vosselman, G., 2000. Slope based filtering of laser altimetry data. *International Archives of Photogrammetry and Remote Sensing*, 33(B3): 935–942.
- Vosselman, G. and H. Mass, 2001. Adjustment and filtering of raw laser altimetry data. *Proceedings of the OEEPE Workshop on Airborne Laser scanning and Interferometric SAR for Detailed Digital Elevation Models*, Stockholm, 1-3, March, 2001.
- Wang, G. X., C. Gertner, P. Parysow and A. Anderson, 2001. Spatial prediction and uncertainty assessment of topographic factor for revised universal soil loss equation using digital elevation models. *ISPRS Journal of Photogrammetry and Remote Sensing*, 56(1): 65-80.
- Wehr A. and U. Lohr, 1999. Airborne laser scanning—an introduction and overview. *ISPRS Journal of Photogrammetry and Remote Sensing*, 54(2-3): 68-82.
- Yoon, J. and J. Shan, 2002. Urban DEM generation from raw airborne LiDAR data. *ASPRS Annual Conference* (CD-ROM), Washington, DC, April 19–25, 2002.